

CALE simulation of Richtmyer-Meshkov instability experiments at high Mach number

A. Miles^{1,2}, J. Edwards¹, G. Glendinning¹

¹Lawrence Livermore National Laboratory

²University of Maryland at College Park

8th International Workshop on the
Physics of Compressible Turbulent Mixing
Pasadena, CA
Dec 9-14, 2001

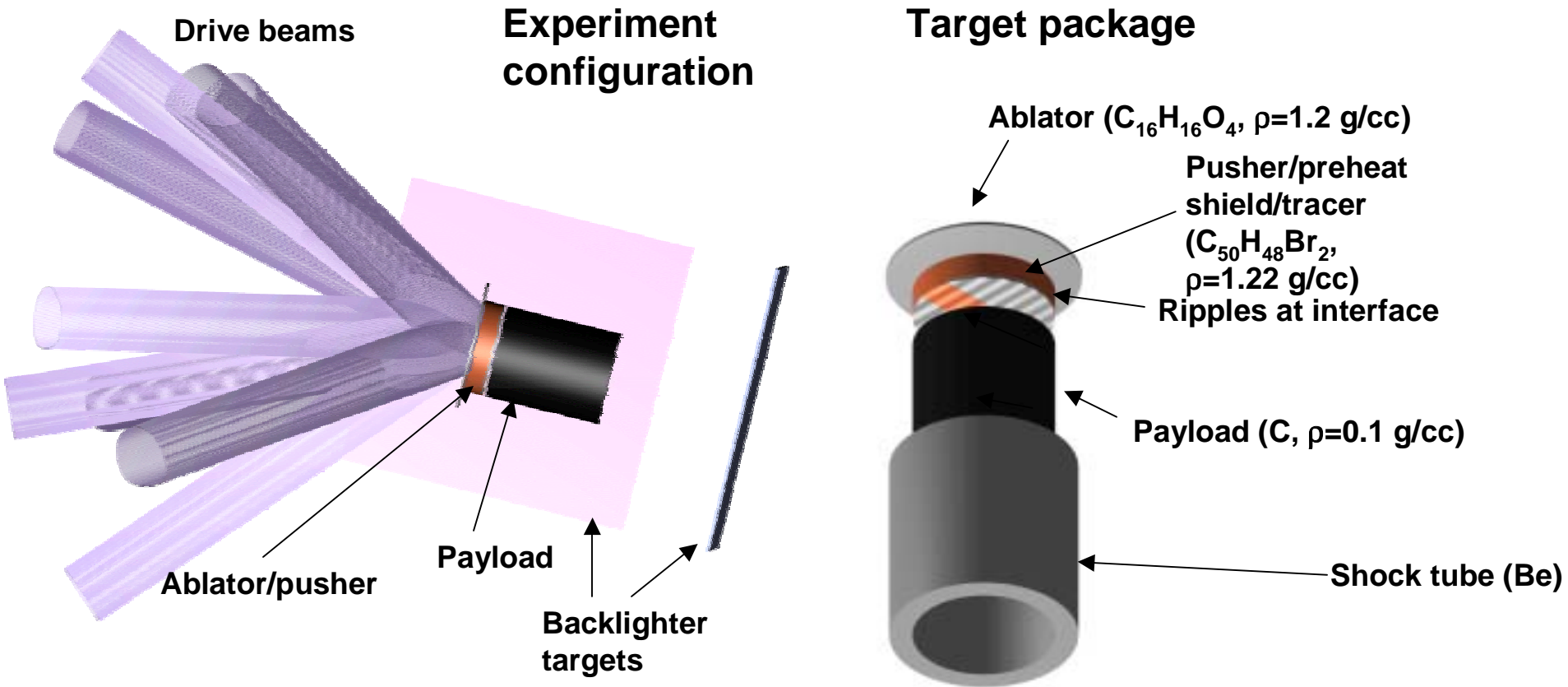
Experiment:

- Omega laser used to generate a strong shock ($M \approx 10$) in a plastic pusher
- Shock drives a corrugated plastic - foam interface ($ka = 0.92$) at near constant velocity
- Richtmyer-Meshkov instability produces growth of the initial perturbation

Simulation:

- C-based Arbitrary Lagrangian-Eulerian (CALE) used to simulate the experiments
- Discrepancies between experiment and simulation are investigated

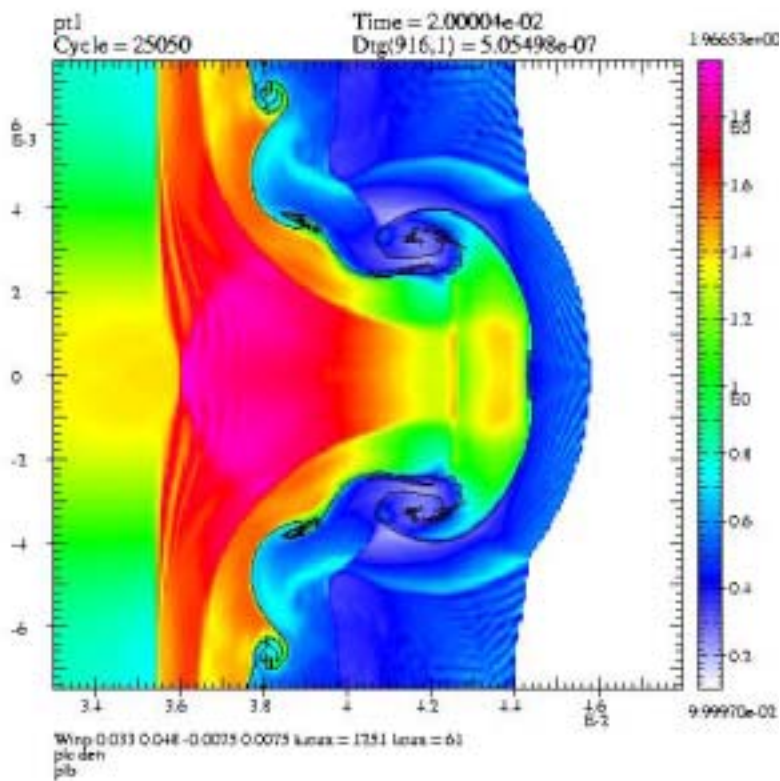
This experiment uses an 11 ns laser drive to create a steady shock incident on a modulated interface



- Backlighting is done on two axes, along target axis and perpendicular to modulations
- Target package is encased in a beryllium shock tube
- The incident shock and interface velocities are constant within $\pm 5\%$ RMS
- The shock is incident on a 12:1 density contrast
- The interface position is measured by side-on radiography

Computational Parameters (CALE)

- $\rho_{\text{plastic}} = 1.1 \text{ g/cc}$
- $\rho_{\text{foam}} = 0.1 \text{ g/cc}$
- $\rho_{\text{void}} = 0.001 \text{ g/cc}$
- $a = 22 \text{ }\mu\text{m}$
- $\lambda = 150 \text{ }\mu\text{m}$
- Computational grid dimensions: $\lambda / 2 \times 700 \text{ }\mu\text{m}$
- With EOP EOS:
 - $c_{\text{plastic}} = 1.84 \text{ }\mu\text{m/ns}$
 - $c_{\text{foam}} = 0.11 \text{ }\mu\text{m/ns}$
 - $P_{\text{plastic}} = 728 \text{ barr}$
 - $P_{\text{foam}} < 1 \text{ barr}$

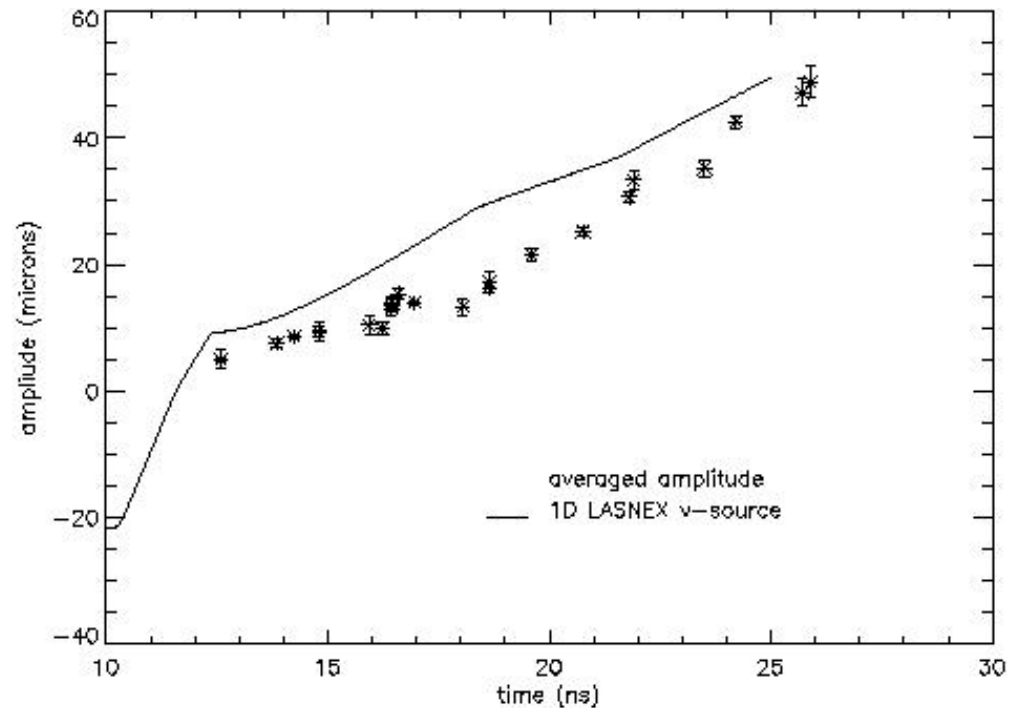
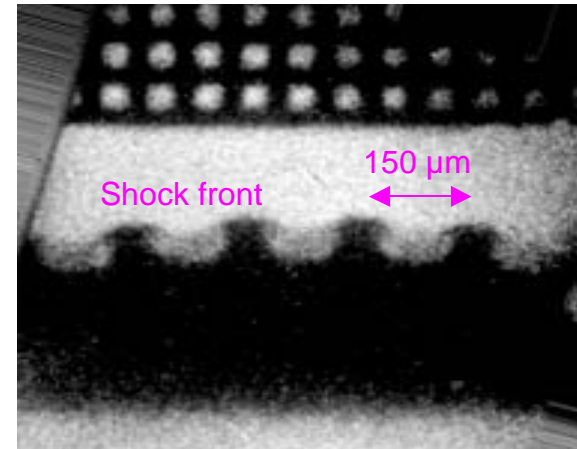


$T = 20 \text{ ns}$

Discrepancies between experiment and simulation:

1. Post-shock amplitude a^* is much too large in simulation - $9 \mu\text{m}$ instead of $5 \mu\text{m}$.
2. Growth rate from 14 - 18 ns is higher in simulation than experiment.
3. The standoff distance of the shock from the interface is larger in the simulation than in the experiment.

Typical side-on data
at 20 ns



Zoning

Two grid configurations used:

- Rectangular grid

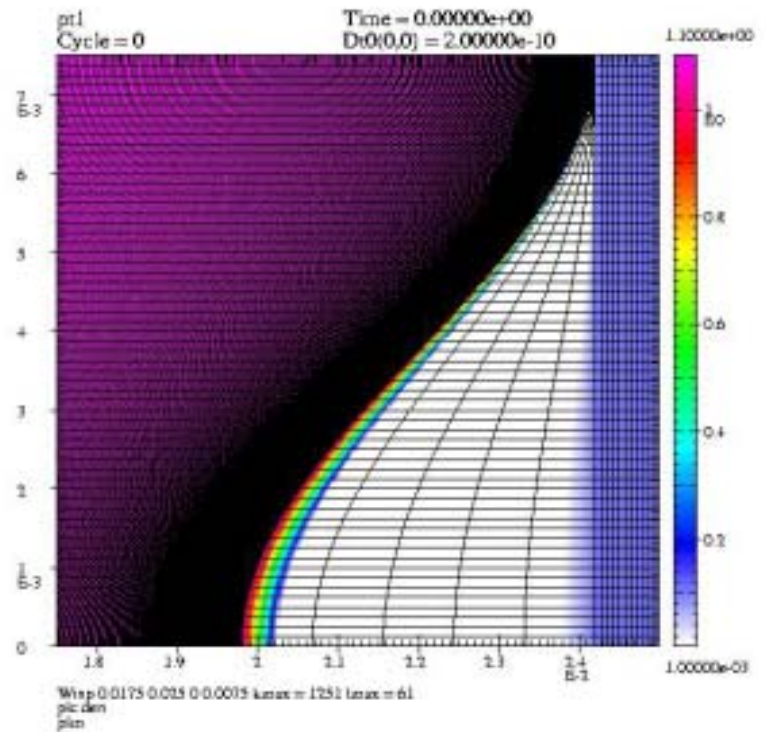
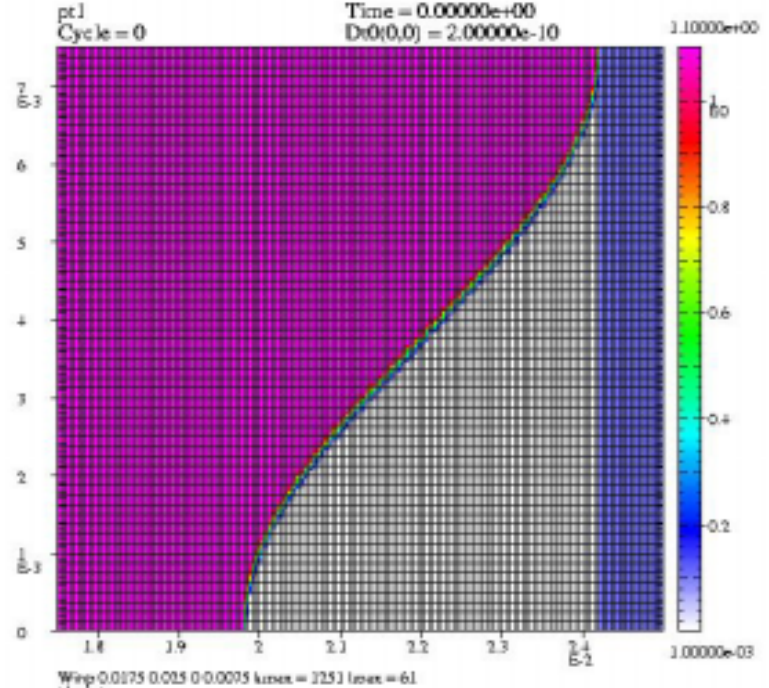
Typical parameters:

- 120 cells/wavelength
1.25 $\mu\text{m}/\text{cell}$
- Cell dimensions:
1.25 μm x 0.5 μm

- Conforming mesh

Typical parameters:

- 120 cells/wavelength
- Plastic and foam “interface”
68% mass-matched
 - 0.1 $\mu\text{m}/\text{cell}$ at plastic-void interface
 - 0.75 $\mu\text{m}/\text{cell}$ at void-foam interface

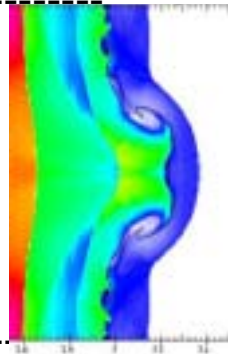


Zoning Effects* I: Conforming Mesh

Cells/wavelength	Cell width across interface (μm)	a^* (μm)	a (25ns) (μm)
------------------	---	-------------------------	------------------------------

120	$0.1 - \Delta_{\text{void}}/5 - 0.75$	10	41
-----	---------------------------------------	----	----

15 ns

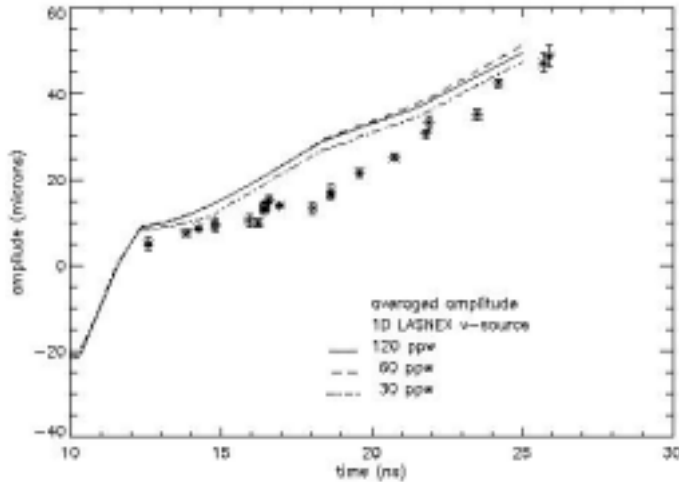


120	$0.01 - \Delta_{\text{void}}/5 - 0.1$ (plastic and foam mass-matched at interface)	11	45
-----	--	----	----

240	$0.01 - \Delta_{\text{void}}/5 - 0.1$	12	47
-----	---------------------------------------	----	----

When the number of cells/wavelength ≤ 240 , a “dimple” forms in the center of the spike. This yields a smaller amplitude, which is defined as half the distance from bubble tip to spike tip. A further increase of cells/wavelength to 480 looks identical to the 240 case, suggesting convergence by 240.

Zoning Effects II: Rectangular Grid



Cells/wavelength

Cell dimensions (μm)

120

1.25 x 0.5

60

2.50 x 1.0

30

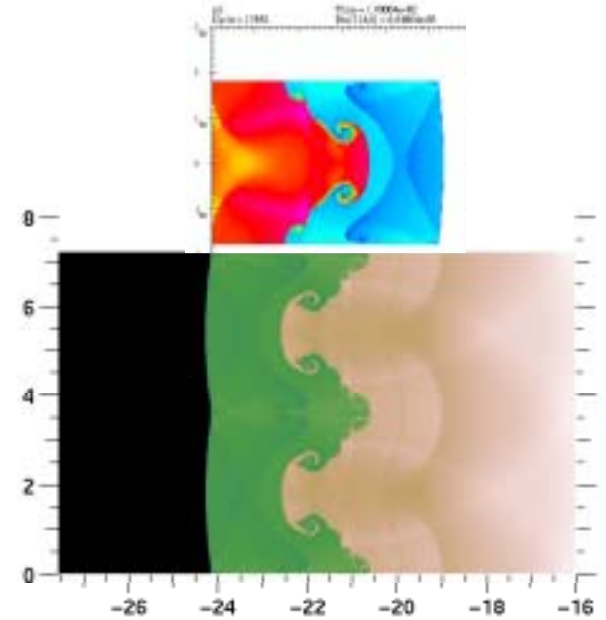
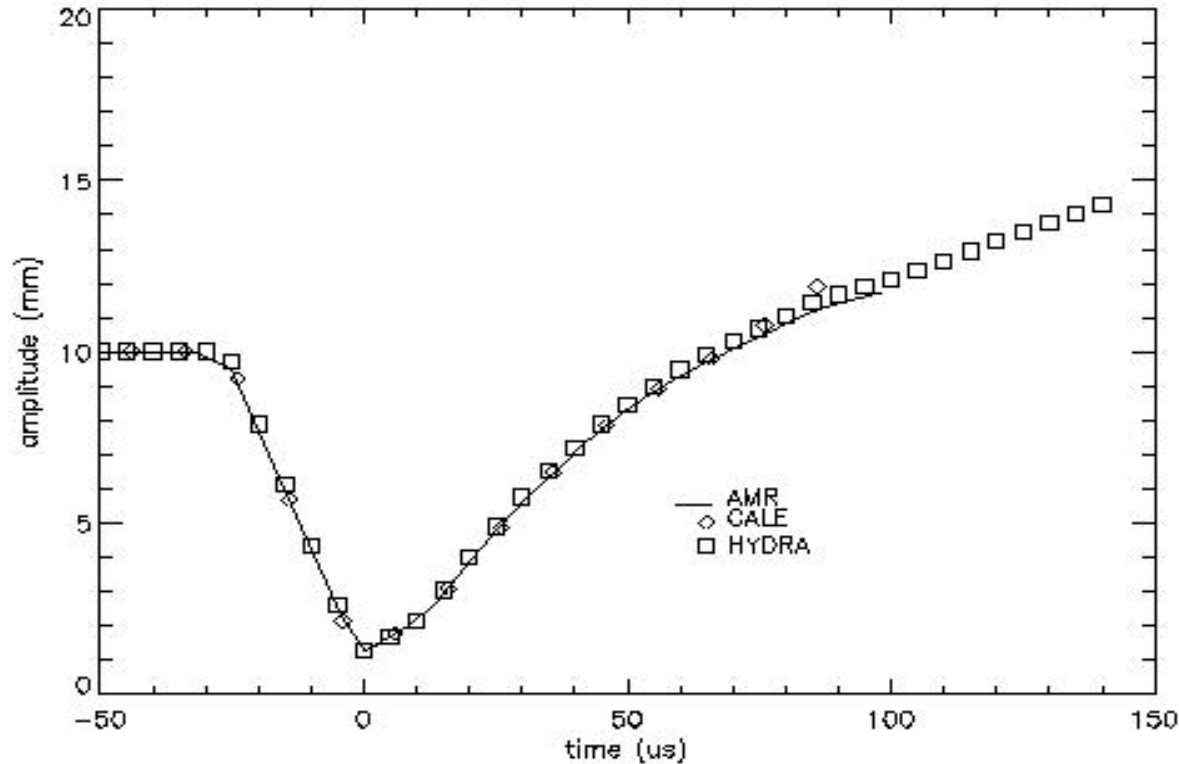
5.00 x 2.0

Further increase of cells/wavelength to 240 looks identical to the 120 case, suggesting convergence by 120.

Beyond 15 ns, the converged conforming and rectangular zoning schemes show virtually identical growth rates. The post shock amplitude a^* is about $1.5 \mu\text{m}$ lower here than in the converged conforming mesh case, and the growth rate at early times is slightly smaller. In what follows, the above grid is used unless otherwise specified.

A one-dimensional study of the effects of cell size for zones mass-matched across the plastic-foam interface shows virtually no change in interface position $z_i(t)$ when the cell size in the plastic at the plastic-void interface is varied from $0.1 - 0.001 \mu\text{m}$. Over this range, $z_i(t)$ is also shown to be insensitive to whether CALE is run in pure lagrangian mode or lagrangian-eulerian hybrid mode.

Comparison of simulations of Aleshin experiment

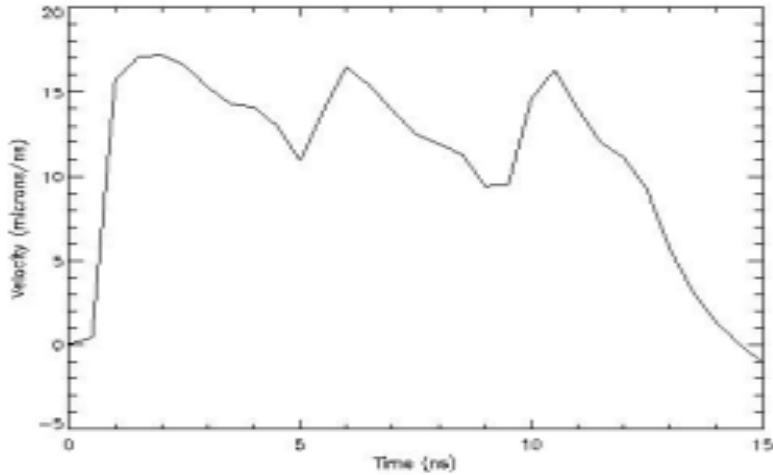


HYDRA (below) and CALE (above) at approx. 80 μs

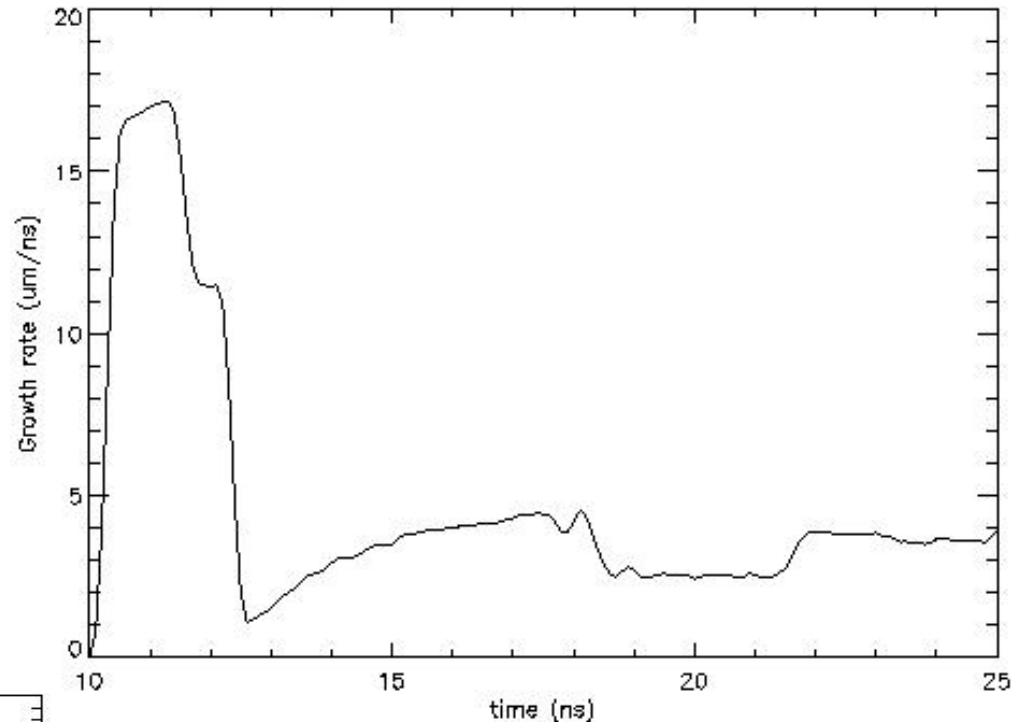
Gas-tube experiment with $M = 4.5$ shock across Xe-Ar interface with $\rho_{Xe} = 2.95$ g/l, $\rho_{Ar} = 2.95$ g/l ($\rho_{Xe} / \rho_{Ar} = 0.30$), $ak = 1.75$

- AMR (Greenough, 2001) and ALE (CALE and HYDRA (Weber, 2001)) simulations of the Aleshin experiment (Aleshin et al., 1996).
- The RAPTOR and HYDRA simulations include 2560 and 512 cells/wavelength, respectively. The CALE simulation was run with only 120 cells/wavelength.
- Despite differences in coarseness, the three simulations show very good agreement in their predictions of amplitude history, and all three are in good agreement with the experimental data (not shown).
- The number of cells/wavelength and the initial ratio of cell dimensions (cell width along / perpendicular to the unperturbed interface) in the above CALE simulation is 2.5 - the same as in simulations of the Omega experiments.

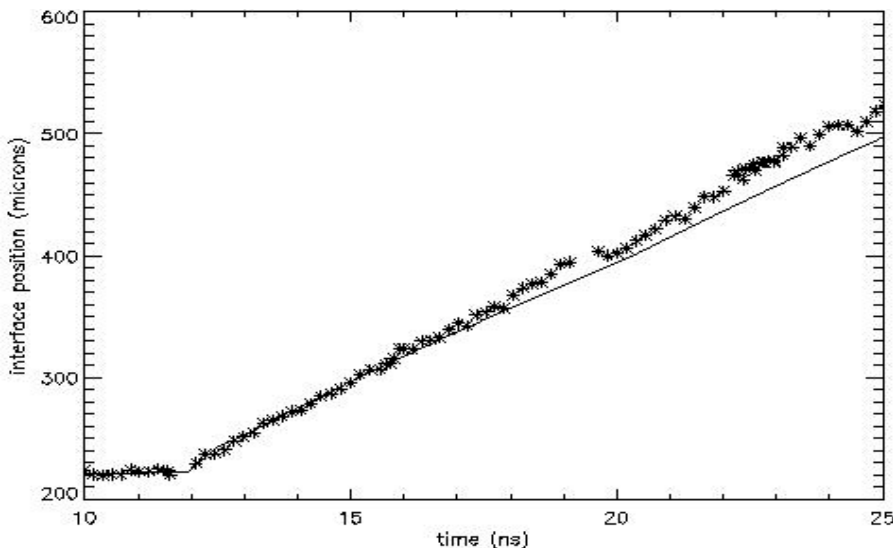
Velocity Source I



A 1D Lasnex simulation translates the 11 ns laser pulse into a velocity source. The result is used as a source input for CALE.

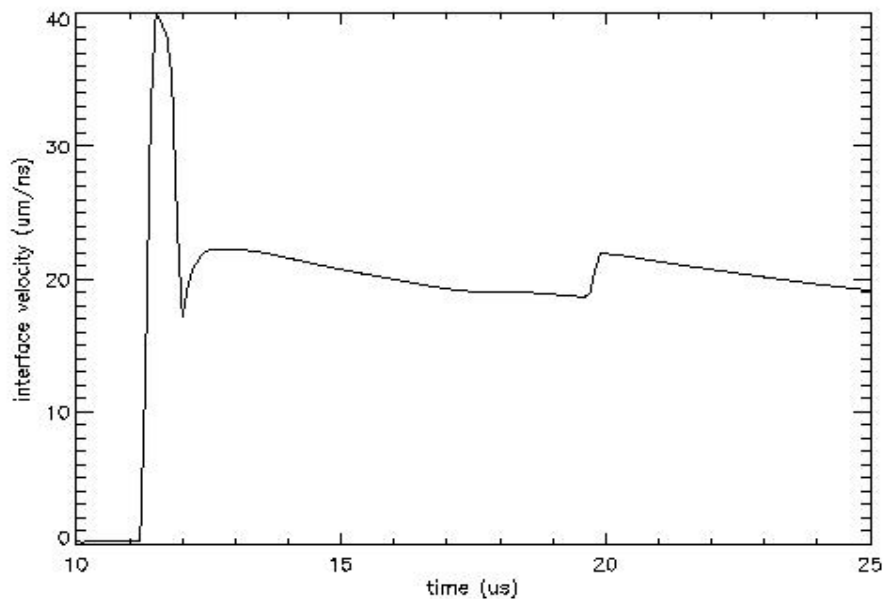


The RM instability growth rate is obtained by numerically differentiating the averaged amplitude history.

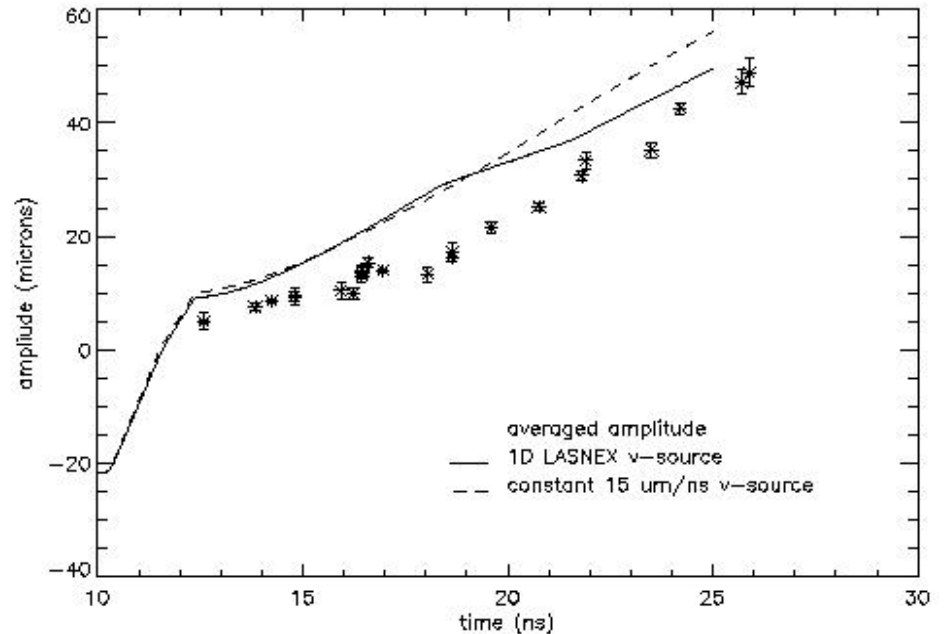


The interface position is obtained from a 1D CALE simulation. The CALE-predicted interface velocity is apparently smaller than in the experiment.

Velocity Source II

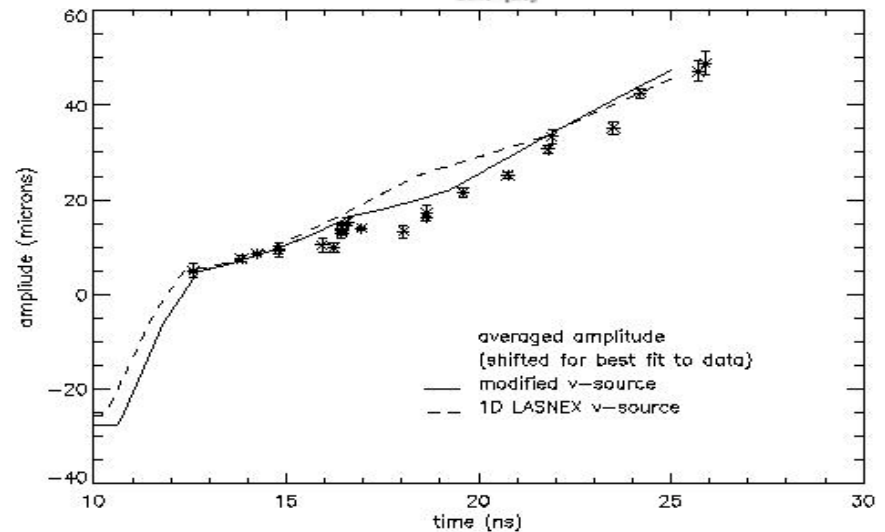
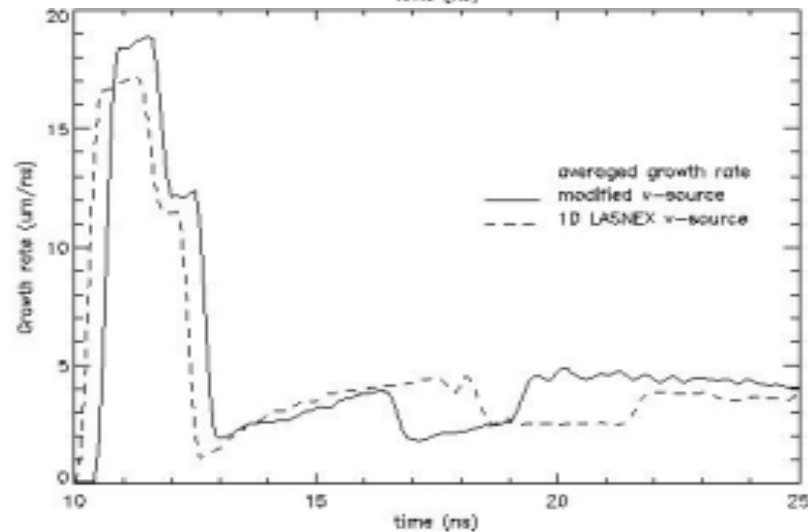
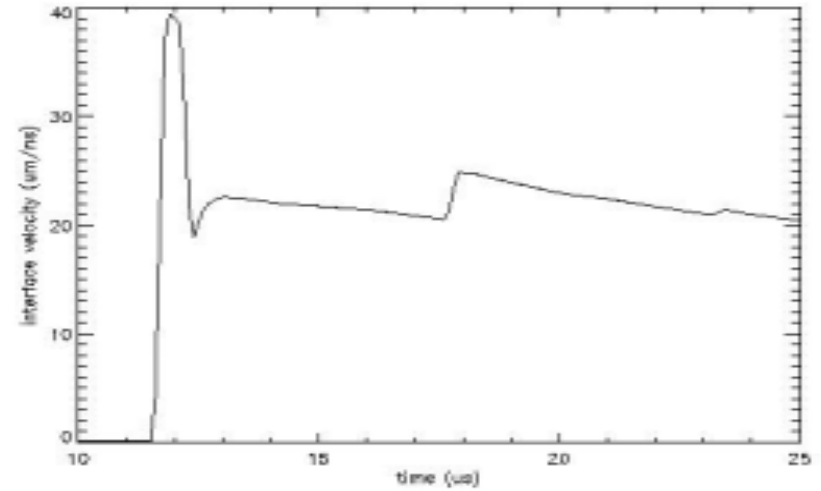
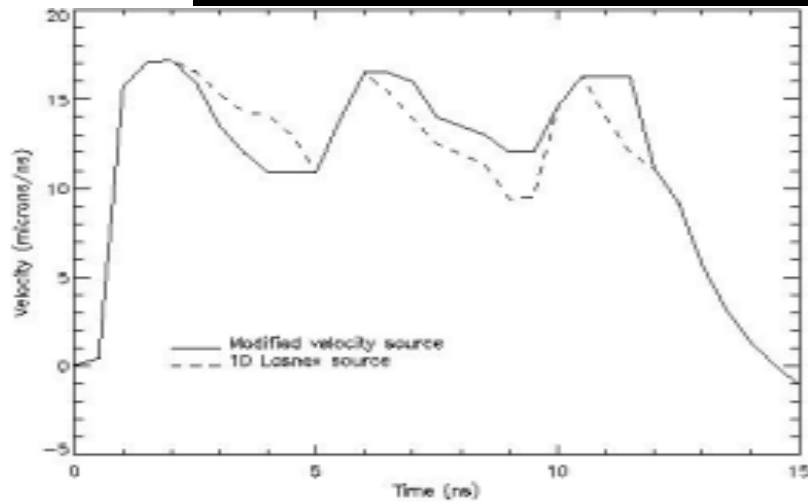


The interface velocity $u_i(t)$ is obtained by differentiating the interface position. It shows that the reduction in growth rate from 18-22 ns corresponds to the arrival at the interface of a second shock. Investigation of modified velocity sources has demonstrated that this second shock corresponds in turn to the third peak in the velocity source.



Effect of velocity source details on amplitude history. The instability develops initially as if driven by a constant velocity ($15 \mu\text{m/ns}$) piston. The two histories diverge significantly only upon the arrival of the second shock at the bubble. The shock associated with the second peak in the velocity source has overtaken the incident shock just before the beginning of the interaction.

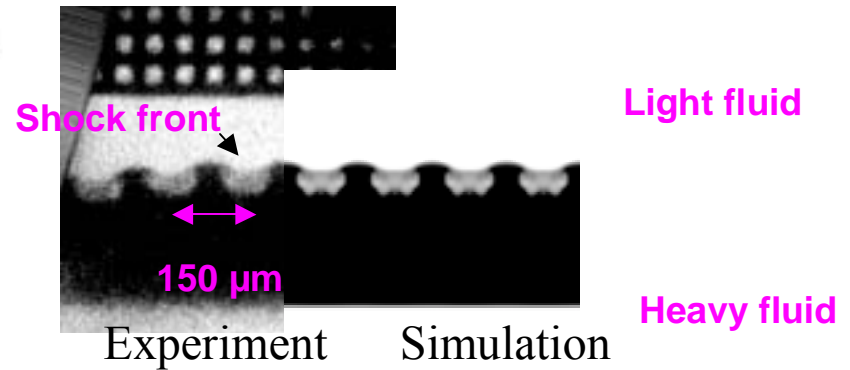
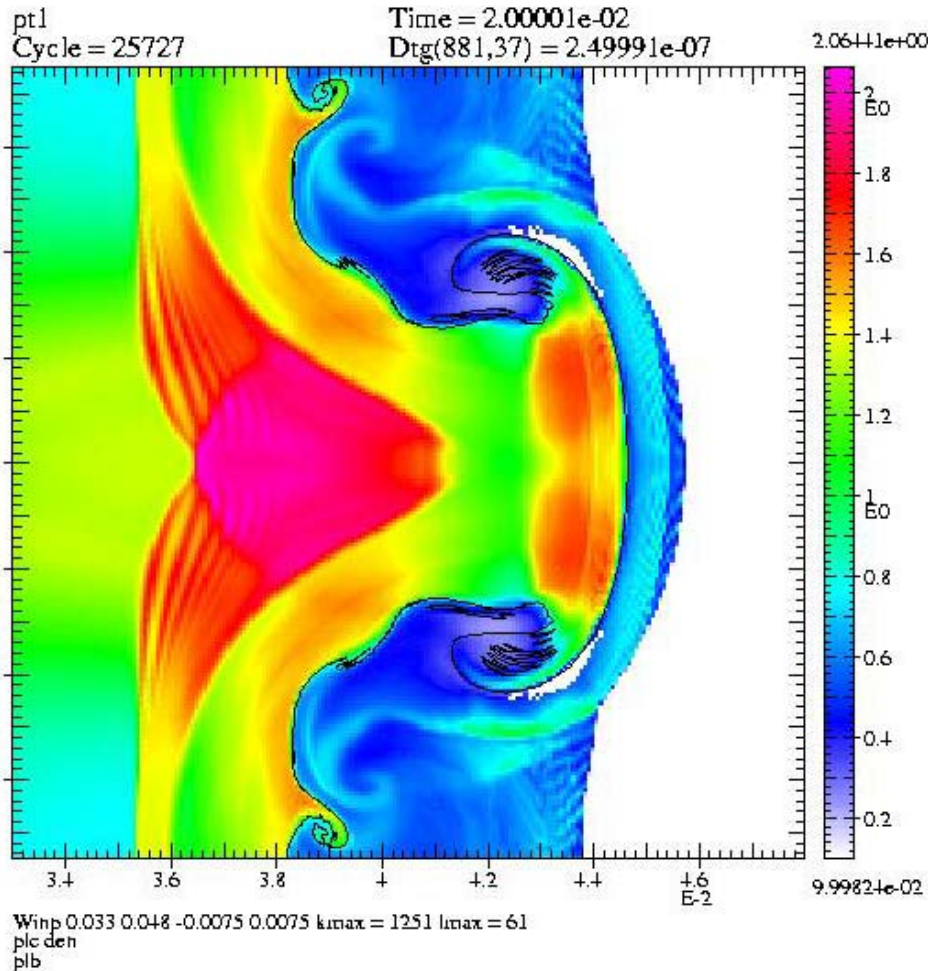
Modified Velocity Source I



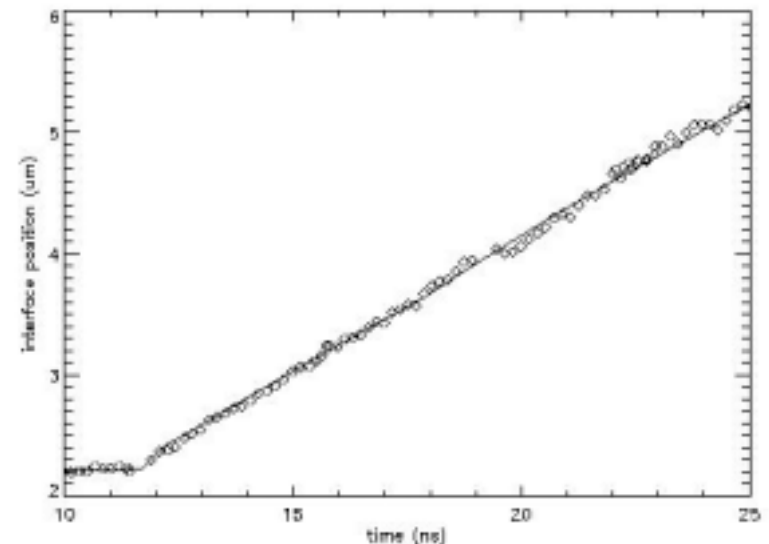
Small changes in the velocity source strengthen the second shock and decrease its arrival time. The resulting amplitude history more closely matches the experimental data.

However, the post-shock amplitude is further increased to 11 μm (from 9 μm).

Modified Velocity Source II

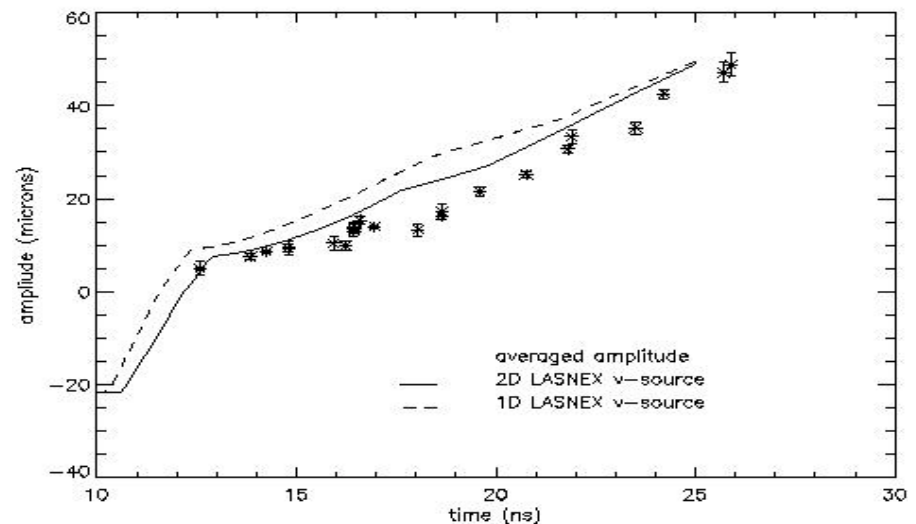
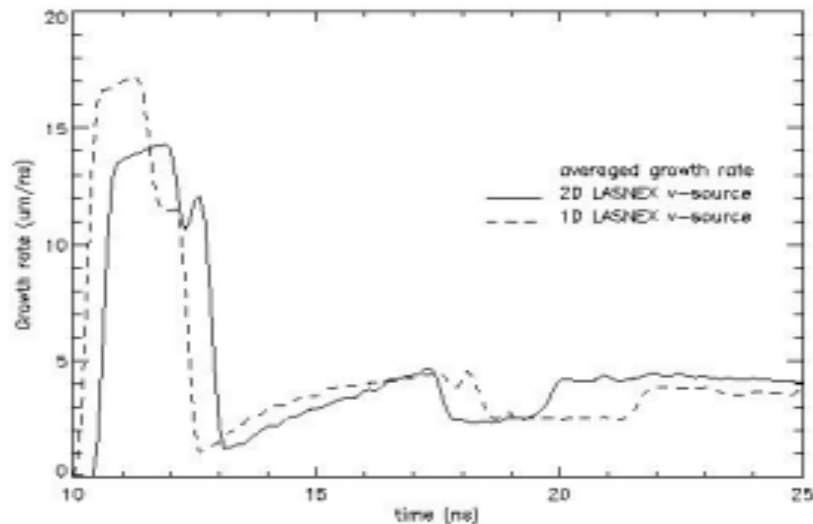
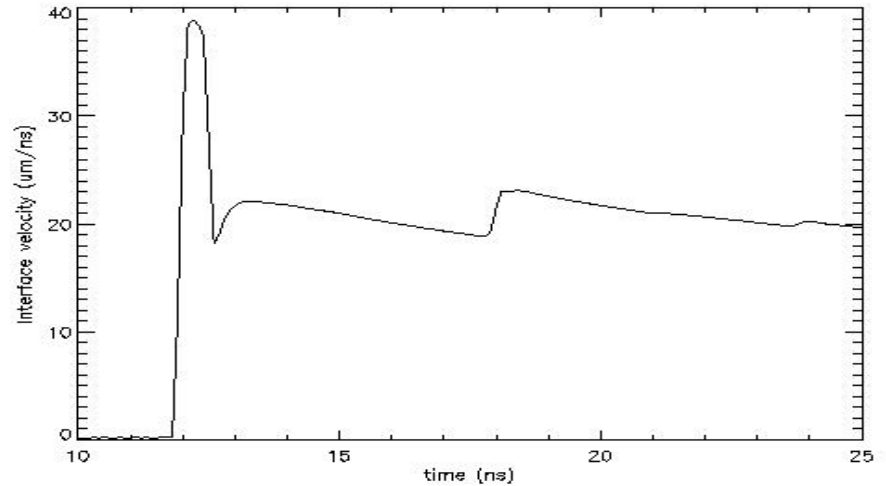
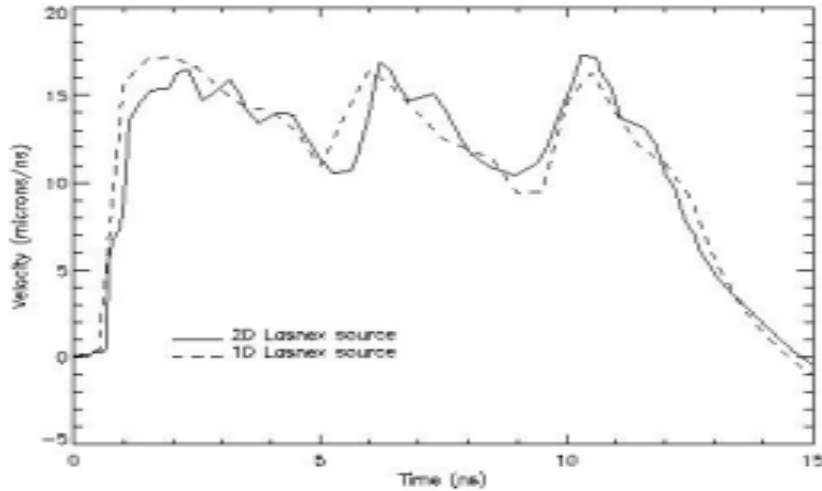


Comparison of simulated x-ray radiograph with experimental x-ray snapshot at 20 ns shows very good agreement.



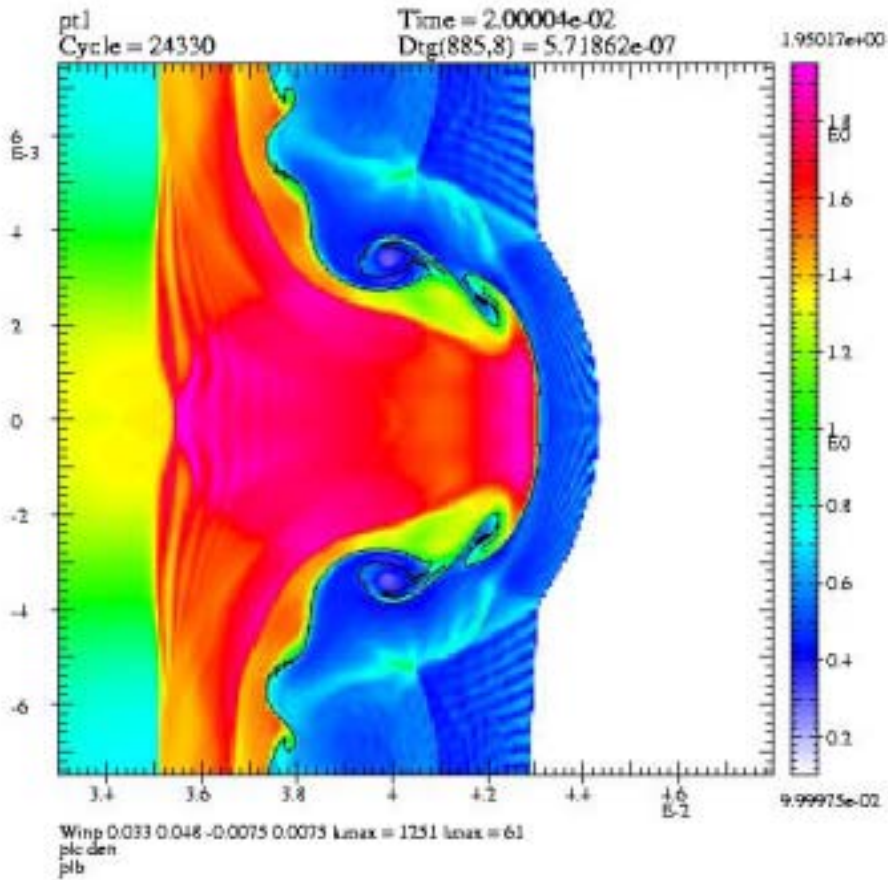
The time-dependent interface position (from 1D CALE simulation) agrees well with experimental measurements.

2D LASNEX Velocity Source I

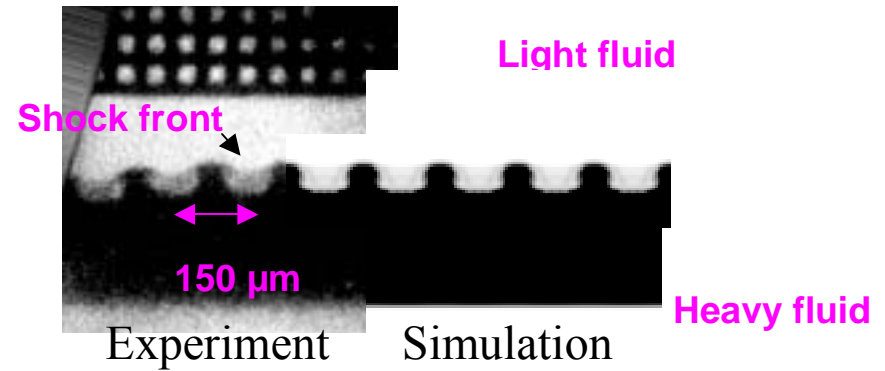


A 2D LASNEX simulation produces a velocity source that differs slightly from the 1D LASNEX prediction. The average interface velocity is increased from $20.4 \mu\text{m/ns}$ to $21.0 \mu\text{m/ns}$. The resulting amplitude history more closely matches the experimental data. Notably, the post-shock amplitude is decreased to $7.7 \mu\text{m}$ (from $9 \mu\text{m}$).

2D LASNEX Velocity Source II

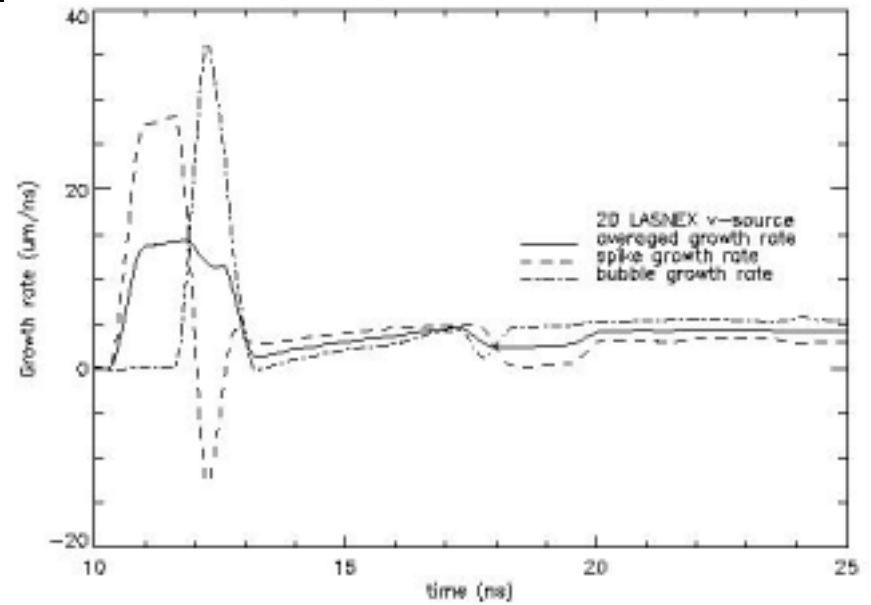
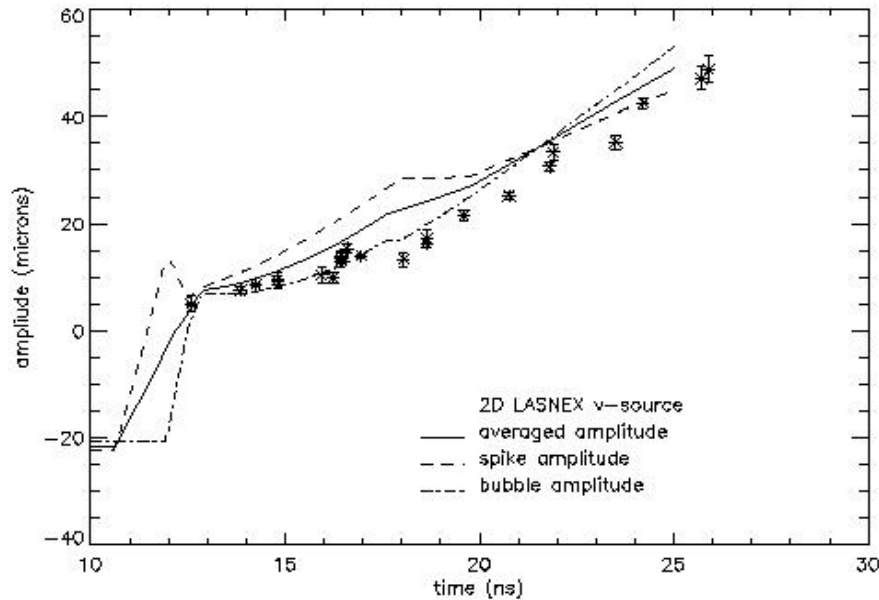


Density plot at 20 ns.

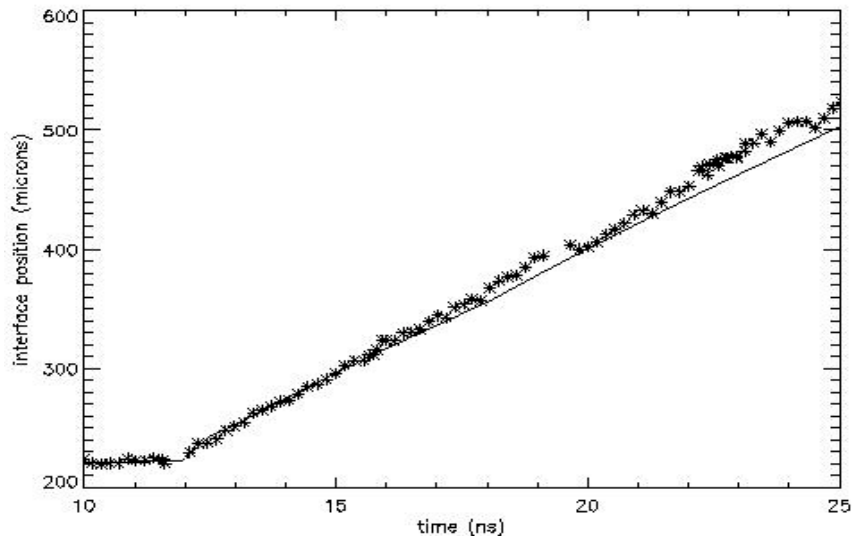


Comparison of simulated x-ray radiograph with experimental x-ray snapshot at 20 ns shows good agreement. However, the CALE-predicted shock is flatter than in the experiment.

2D LANSEX Velocity Source III

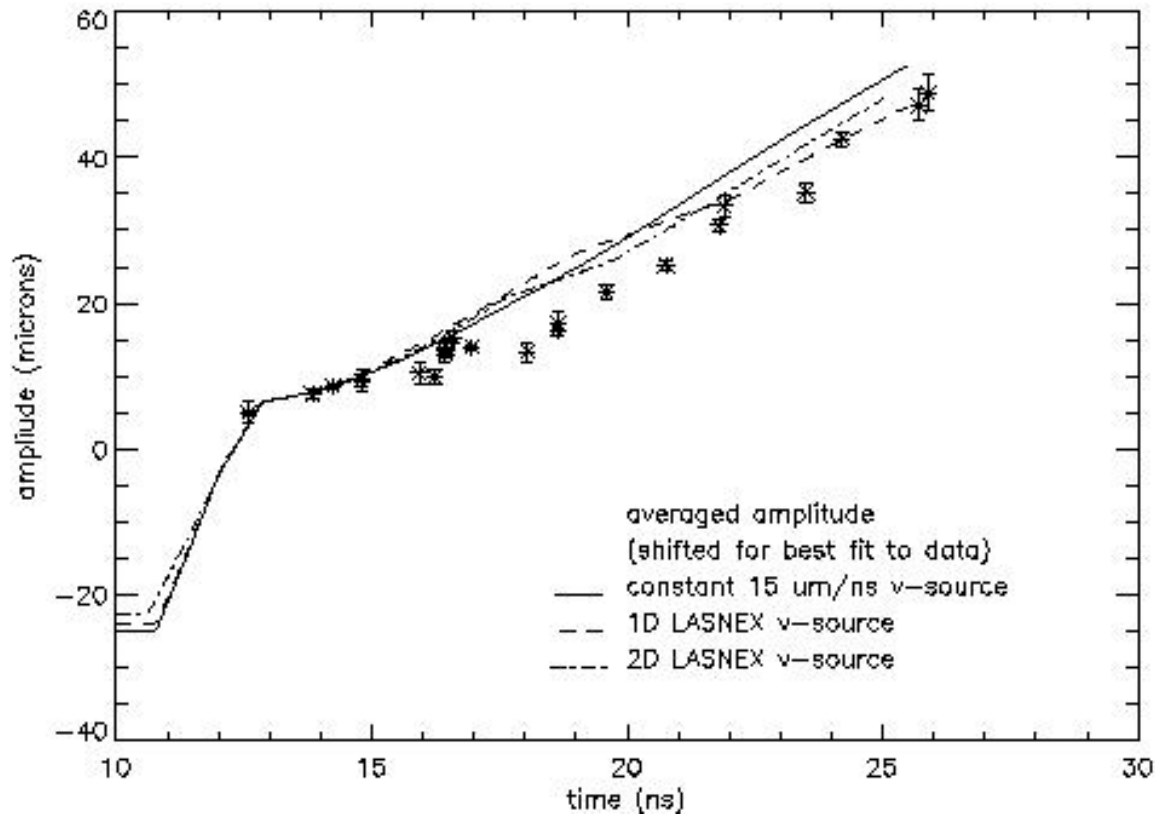


Separate spike and bubble amplitudes and growth rates. The reference time-dependent interface position is obtained from a 1D simulation including a $22\ \mu\text{m}$ gap separating the plastic and foam regions.



The time-dependent interface position (from 1D CALE simulation) is shown to agree well with experimental measurements at early times. After 15 ns, however, the interface velocity is too low.

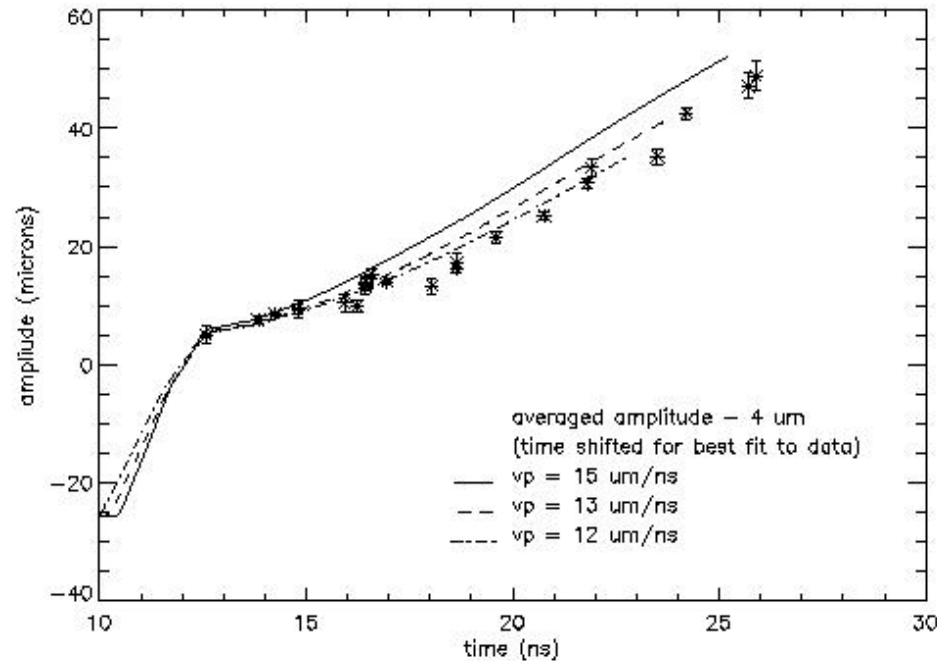
2D LASNEX Velocity Source IV



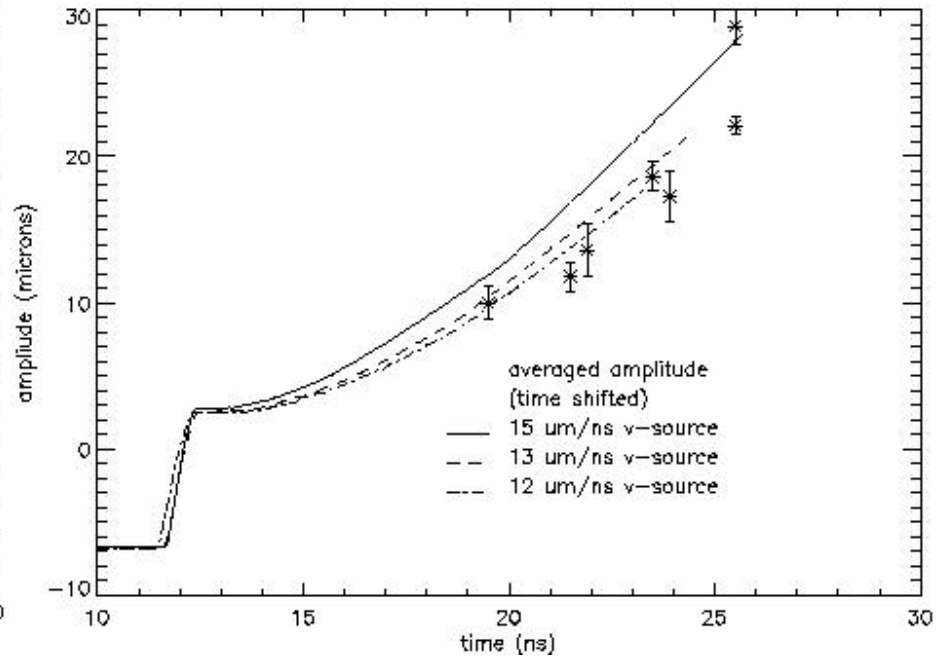
2D LASNEX: t , a - 1.0 μm ; 1D LASNEX: $t + 0.5$ ns, a - 2.5 μm ; Flat source: $t + 0.5$ ns, a - 3.5 μm

Aside from a shifts in time and amplitude, the constant velocity 15 $\mu\text{m}/\text{ns}$ velocity source provides early time instability growth that agrees well with the 2D as well as 1D LASNEX v-source.

Effect of Pusher Velocity



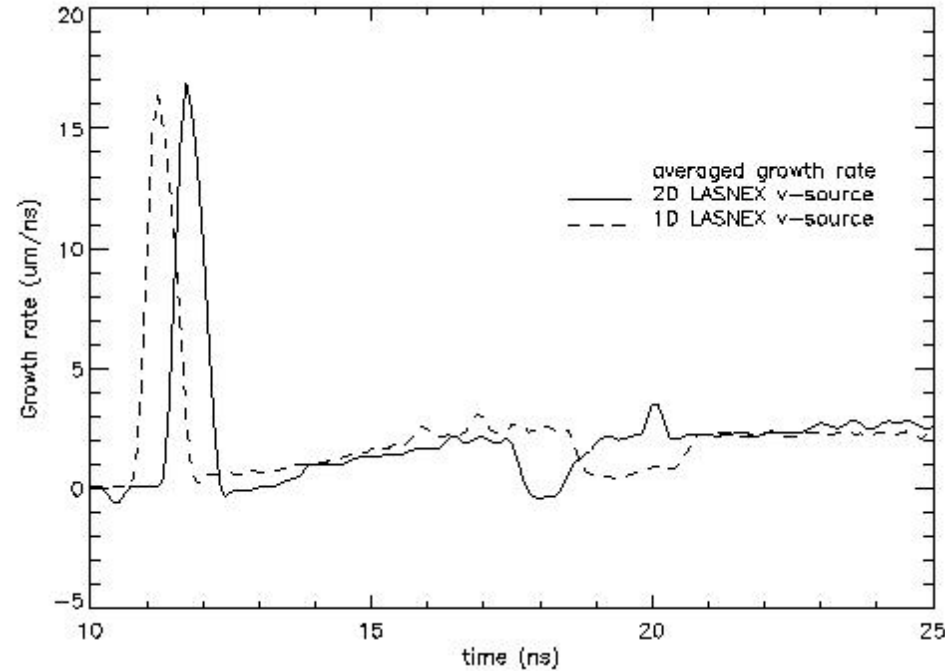
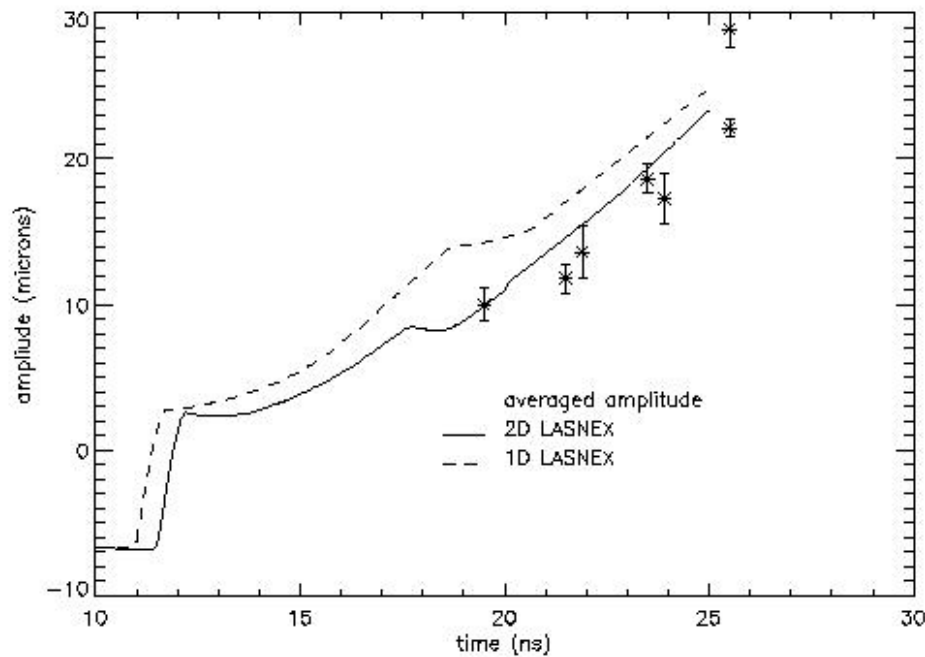
22 μm initial amplitude



7 μm initial amplitude

The post-shock amplitude is insensitive to the piston velocity over a range of several $\mu\text{m/ns}$. For comparison, the average velocities of the 1 and 2D Lasnex v-sources from 1 - 11 ns are 14.0 and 13.9 $\mu\text{m/ns}$, respectively. The analogous averages taken from the first to the second peak in the velocity profiles are 15.0 and 14.1 $\mu\text{m/ns}$.

2D LASNEX Velocity Source V



The simulation with the 2D LASNEX velocity source is also in closer agreement with experimental data obtained from experiments with small initial perturbation amplitude ($a = 7 \mu\text{m}$, $ka = 0.29$).

Equation of State I:

Effect on basic parameters, post-shock amplitude, and early-time growth rate
All lengths are in μm , times in ns.

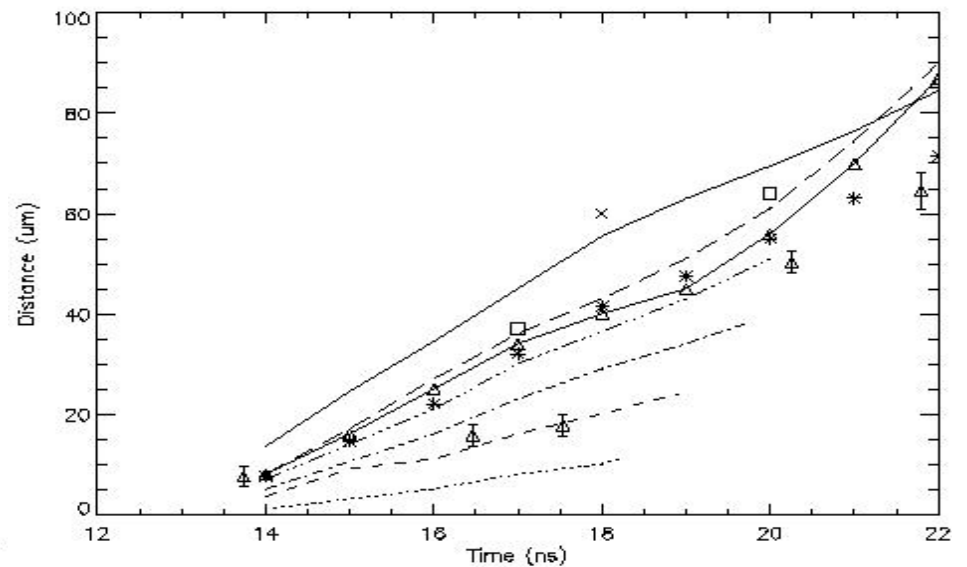
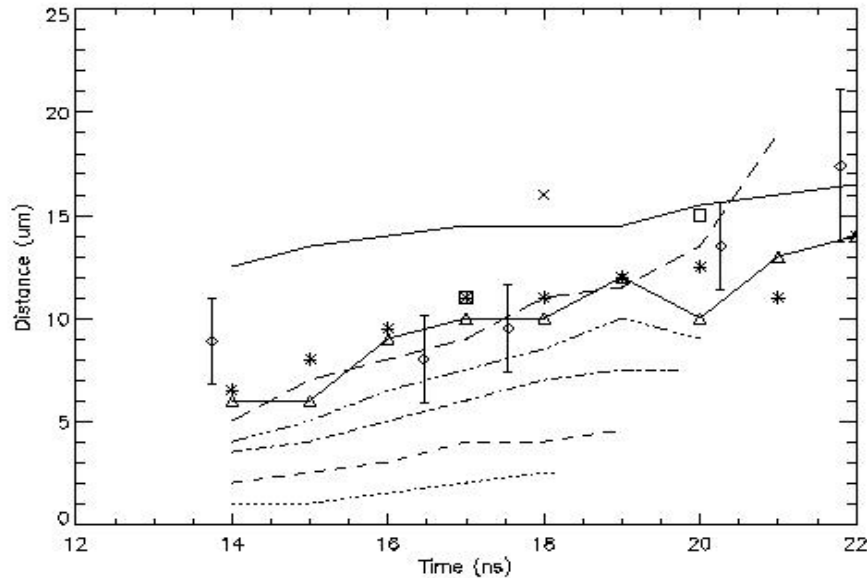
	V_1 (ave 2-8 ns)	γ_1^{eff}	u_i	v_2 (v_2^{rel})	γ_2^{eff}	a^*	da/dt ave($t^* - 18\text{ns}$)	$da/dt^{\dagger\dagger}$
Exp	22.0 ± 0.2	1.93 ± 0.03	21.9 ± 1	26.1 ± 0.5 (4.2)	1.38	5.0	$\approx 1.9 \pm 0.1$	
EOP-1D [†]	20.9	1.80	20.4	25.1 (4.7)	1.46	9.0	3.4	4.3
EOP-2D [†]	20.8		21.0	26.1 (5.1)		7.7	3.0	4.5
EOP	19.6		22.2	27.0 (4.8)		10.5	2.8	4.0
LEOS	18.9	1.67	22.9	29.4 (6.5)	1.66	13.0	3.1	4.5
γ/EOP		1.5				13.5		2.1
γ/EOP		1.9				11.0		4.9
γ/EOP		2.0				7.0		5.0
γ/EOP		2.2				7.0		5.5
EOP/ γ					1.1	11.0		3.2
EOP/ γ					1.2			3.5
EOP/ γ					1.3			3.8
EOP/ γ					1.4			3.9
EOP/ γ					1.5	10.5		4.0

[†]Simulation run with drive from LASNEX calculation - all others run with modified v-source.

^{††} Peak growth rate over interval from t^* , defined by $a(t^*)=a^*$, to instant where second shock reaches the bubble front.

v_2^{rel} is shock speed in interface frame

Equation of State II: Shock Proximity



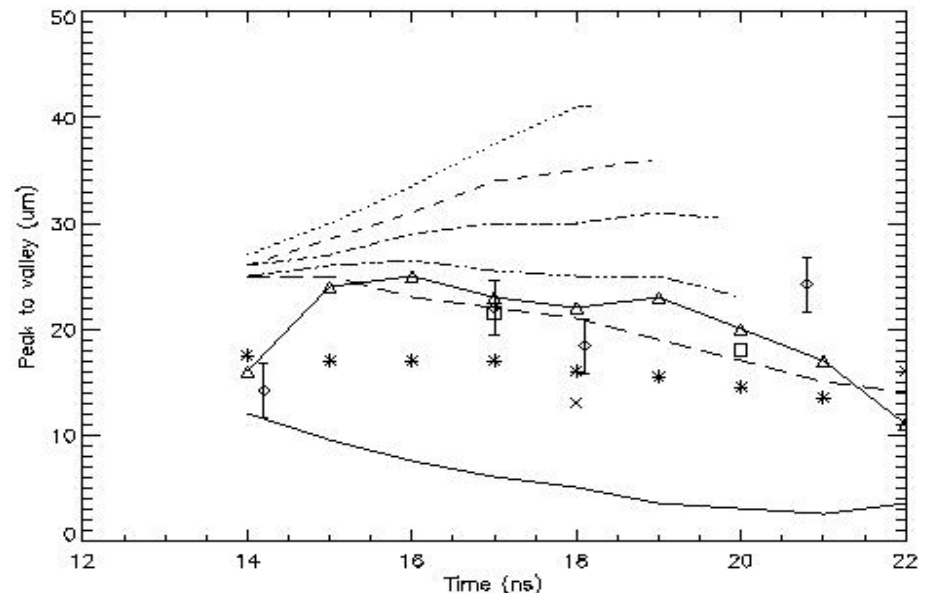
Distance from spike to shock

Modified v-source and EOP EOS unless otherwise specified

- | | |
|---------------------------------------|---------------------------------------|
| —△— EOP | $\gamma_{\text{fom}} = 1.1$ |
| x LEOS | ----- $\gamma_{\text{fom}} = 1.2$ |
| □ 1D LASNEX v-source | - · - · - $\gamma_{\text{fom}} = 1.3$ |
| * 2D LASNEX v-source | - · · · - $\gamma_{\text{fom}} = 1.4$ |
| — 1D LASNEX v-source, foam-filled gap | ———— $\gamma_{\text{fom}} = 1.5$ |

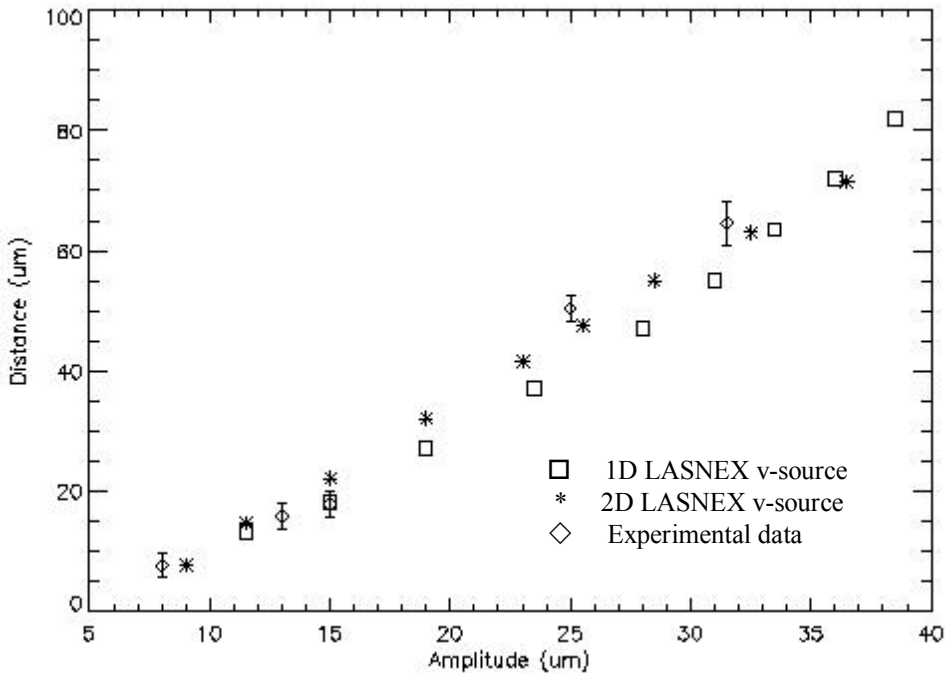
Shock proximity and distortion compared for various EOS models and velocity source profiles. No one combination of EOS model and v-source matches all of the data. The discrepancy between data and experiment on the bubble proximity is generally consistent with the discrepancy in perturbation amplitude.

Distance from bubble to shock

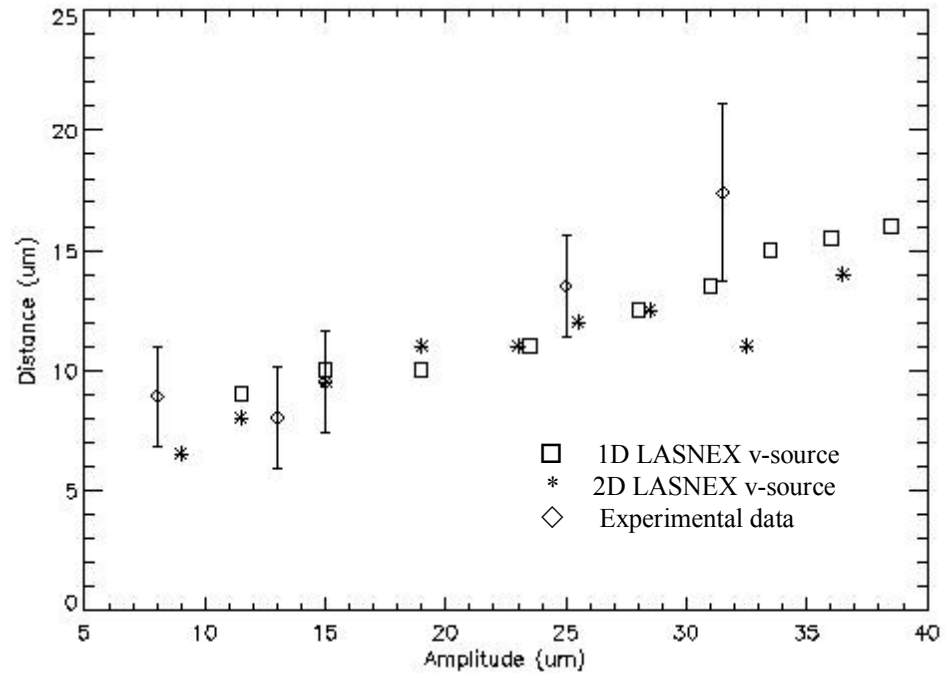


Shock distortion

Shock-Proximity vs Amplitude



Distance from bubble to shock



Distance from spike to shock

Post-shock amplitude

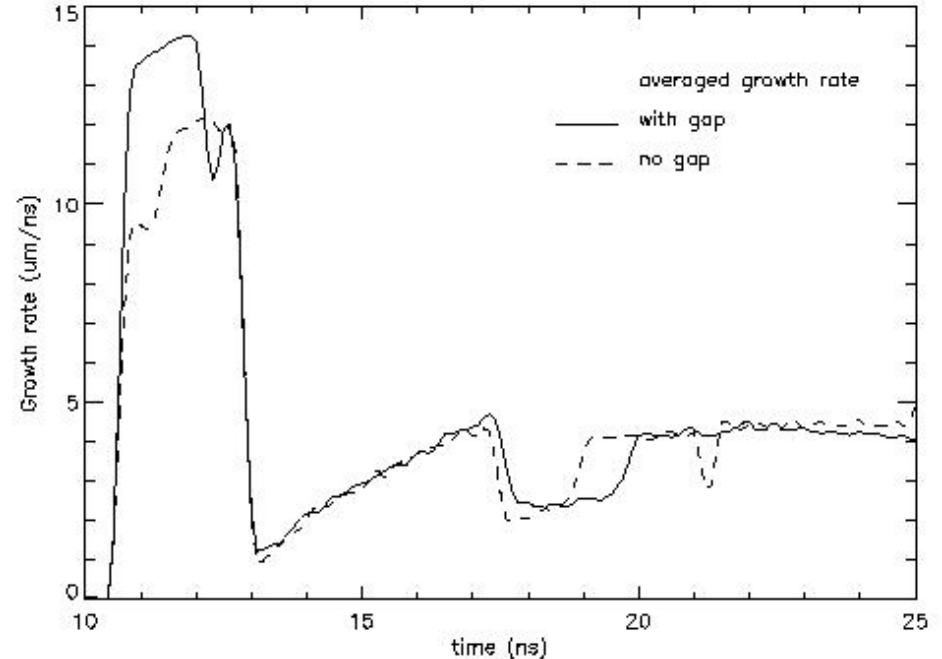
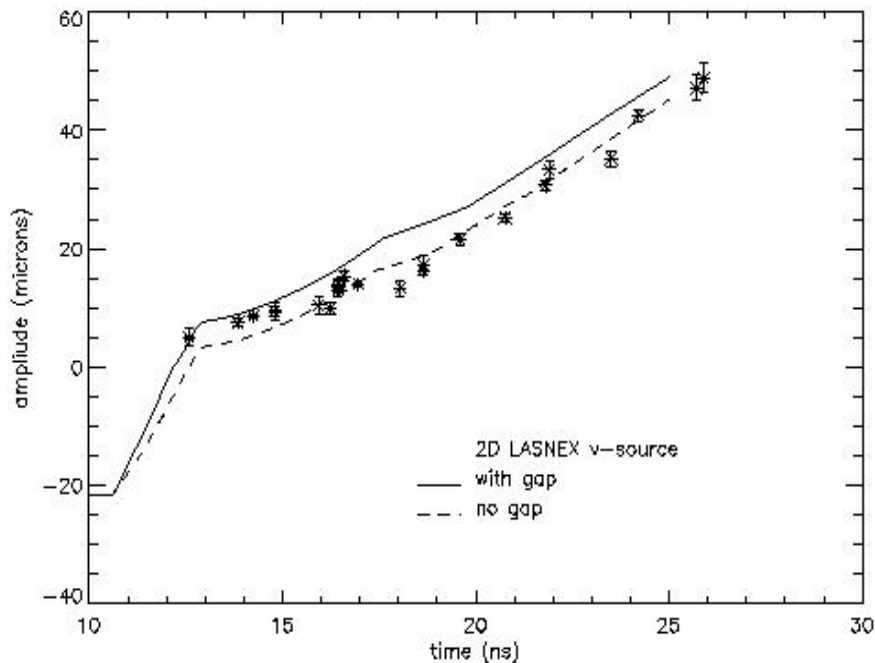
- a^* has been shown to exhibit only weak dependence on EOS and zoning issues.
- a^* is defined by half the bubble to spike distance at the instant the shock completely crosses the interface, and is determined by the compression factor:

$$\frac{a^*}{a} = u_i \frac{1}{v_1} - \frac{1}{u_g}$$

Where u_i is the interface velocity, v_1 is the shock speed in the plastic, and u_g is the interface velocity in the gap. This reduces to the usual expression in the absence of a gap, when $u_g = u_i$.

- For the reported experimental amplitude and velocity values, this requires $u_g = 28.5 \pm 1.3 \mu\text{m/ns}$. If the incident shock and interface velocities at the time of interaction are used (rather than their average values), we find $u_g = 26.5 \mu\text{m/ns}$. A rough measurement from the data suggests $u_g = 20 \pm 10 \mu\text{m/ns}$. The analogous calculation for the simulations with an EOP EOS gives $u_g = 33.9 \mu\text{m/ns}$ (modified v-source), $u_g = 36.0 \mu\text{m/ns}$ (1D LASNEX v-source), and $u_g = 31.8 \mu\text{m/ns}$ (2D LASNEX v-source), while, for LEOS, $u_g = 36.9 \mu\text{m/ns}$ (modified v-source). The actual values from the three simulations are 37 ± 1 , 34 ± 1 , 28 ± 1 and $40 \pm 1 \mu\text{m/ns}$, respectively.

Post-shock Amplitude II: Modified gap



When the gap is “filled in” with foam, the breakout speed of the interface into the gap region is reduced. The speed of the interface in the gap is one-half the instability growth rate until the moment that the incident shock reaches the position of the unperturbed interface. The reduction in breakout speed produces a corresponding reduction in post-shock amplitude.

Conclusions I

- CALE simulations of high Mach number RM experiments have been performed.
- Results obtained using computational grids initially rectangular or conforming agree with one another provided the number of zones/wavelength is sufficiently large. Convergence is obtained more rapidly for rectangular grid.
- Although the general features of the experiments are correctly predicted by the simulations, there are discrepancies.
- The discrepancy between the experimental and simulation a^* does not appear to be caused by EOS issues. It has been shown most sensitively dependent on the details of: the composition of the gap region, the shock-gap dynamics, and the velocity source.

Conclusions II

- Relatively small details of the velocity source can significantly affect the post-shock amplitude and the instability growth rate. CALE simulations in which the input velocity source was obtained from a 2D rather than 1D Lasnex simulation show improved agreement of a^* and $da(t)/dt$ with the experimental data. This is true for both both the large and small amplitude cases.
- The discrepancy between experimental and simulation $da(t)/dt$ from 17 - 20 ns does not appear to be caused by zoning or EOS issues. Simulations with a modified v-source suggest that, in the experiment, the second shock (observed with both Lasnex velocity sources) reaches the perturbation about 1 ns earlier than in the CALE simulation with 2D Lasnex v-source. This in turn suggests that further refinement of the velocity source will be required for more accurate simulations of the experiment.
- The long-term shock proximity observed in the experiments suggests that the foam may more compressible than predicted by the EOP tables, and is certainly more compressible than predicted by the LEOS tables. The degree of shock proximity remains the most significant discrepancy between the experiments and simulations.